Catalysis Today 186 (2012) 115–120

Contents lists available at SciVerse ScienceDirect

Catalysis Today

journal homepage: www.elsevier.com/locate/cattod

High-temperature synthesis of magnetically active and SO_3H-functionalized ordered mesoporous carbon with good catalytic performance

Fujian Liu[b], Jing Sun[c], Qi Sun[a], Longfeng Zhu[c], Liang Wang[c], Xiangju Meng[a], Chenze Qi[b], Feng-Shou Xiao[a],*

[a] Key Lab of Applied Chemistry of Zhejiang Province, Department of Chemistry, Zhejiang University (XiXi Campus), Tianmushan Road 148, Hangzhou 310028, China
[b] Institute of Applied Chemistry, Shaoxing University, Shaoxing 312000, China
[c] State Key Laboratory of Inorganic Synthesis and Preparative Chemistry, College of Chemistry, Jilin University, Qianjin Street 2699, Changchun 130012, China

ARTICLE INFO

Article history:
Received 26 May 2011
Received in revised form 7 November 2011
Accepted 11 November 2011
Available online 9 January 2012

Keywords:
Magnetically active
Ordered mesoporous carbon
Heterogeneous acidic catalysts
Catalyst recyclability

ABSTRACT

Magnetically active and SO_3H-functionalized ordered mesoporous resin and carbon (MOMR-SO_3H, MOMC-SO_3H) were successfully prepared by high-temperature hydrothermal synthesis from resol, copolymer surfactant, and iron cations at 180 °C, followed by sulfonation from sulfuric acid fuming. X-ray diffraction patterns show that MOMR-SO_3H and MOMC-SO_3H have ordered hexagonal mesoporous symmetry. N_2 isotherms indicate that these samples have uniform and opened mesopores, high surface areas (335–591 m^2/g), and large pore volumes (0.34–0.35 cm^3/g). Transmission electron microscopy shows that iron nanoparticles, which are superparamagnetic in nature, are highly dispersed in MOMC-SO_3H sample. Catalytic tests show that MOMC-SO_3H is highly active and excellently recyclable in esterification of acetic acid with butanol, esterification of acetic acid with cyclohexanol, and condensation of benzaldehyde with ethylene glycol. More interestingly, MOMC-SO_3H catalyst is magnetically active, showing potential applications for separating catalysts by a magnetic field in the future.

1. Introduction

The replacement of liquid acids by solid acids is greatly important for the production of fine chemicals recently owing to the obvious advantages of simple separation of the catalysts from the reaction media and significant reduction of environmental pollution [1–12].

Zeolites as typical solid acids have been widely applied due to their high surface area, adjustable framework, and product shape-selectivity [1]. However, the conversion of bulky molecules is not easy in relatively small micropores of zeolites due to the difficulty for access of these bulky molecules to the catalytically active sites [1,2]. Synthesis of ordered materials such as MCM-41 and SBA-15 offers a totally new route to solve the limitation of micropores [13–15], but the amorphous nature of the mesoporous walls normally has weak acidity [1,2]. To achieve strong acidic sites, SO_3H groups have been functionalized on the surface of the mesoporous walls [6,16–20], giving excellent catalytic properties in a series of acid-catalyzed reactions. Notably, compared with zeolites, ordered mesoporous materials including silicas and aluminosilicates have relatively low hydrothermal stability, which strongly limit catalytic applications [21]. To overcome this problem, porous resins and carbons with SO_3H groups have been prepared [22–28]. Particularly, it is worth mentioning that ordered porous resins and carbons could be prepared from self-assembly routes recently [29–32].

To increase activities, SO_3H-functionalized porous carbons are usually used as fine powders in catalysis. However, the separation of the fine powders from catalytic systems is a challenge. Recently, magnetically active composites have been successfully synthesized [33–39], which offer an alternative route for separating fine powders by a magnetic field. Notably, magnetically active nanocrystals of iron oxides are hydrothermally synthesized at the temperatures higher than 140 °C [40], but conventional synthesis of ordered mesoporous materials is generally fabricated at relatively low temperatures (<140 °C) [15].

More recently, it is reported a successful high-temperature synthesis of ordered mesoporous resins at 150–260 °C [41], which shows a possibility for preparing magnetically active porous resins and carbons. In this work, we show a high-temperature synthesis of magnetically active and SO_3H-funcationalized ordered mesoporous carbon (MOMC-SO_3H). Catalytic tests in esterification of acetic acid with butanol, esterification of acetric acid with cyclohexanol, and condensation of benzaldehyde with ethylene glycol show that MOMC-SO_3H has comparable activities and good recyclability, compared with conventional solid acidic catalysts of Amberlyst 15 and SBA-15-SO_3H.

---

* Corresponding author.
E-mail addresses: fsxiao@zju.edu.cn, fsxiao@mail.jlu.edu.cn (F.-S. Xiao).

0920-5861/$ – see front matter © 2011 Elsevier B.V. All rights reserved.
doi:10.1016/j.cattod.2011.11.011

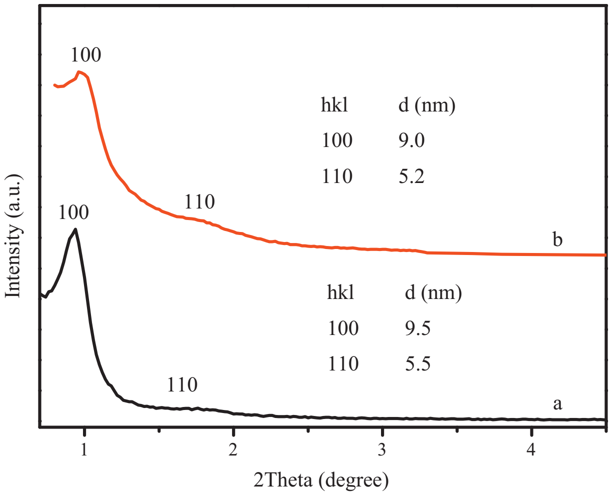

Fig. 1. Small angle XRD patterns of (a) MOMR-SO_3H and (b) MOMC-SO_3H.

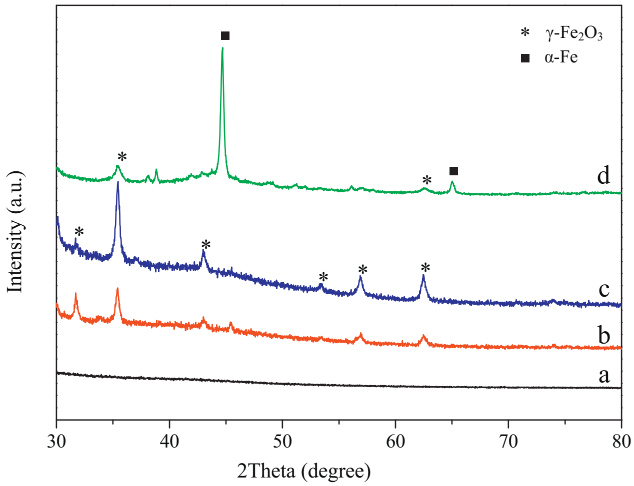

Fig. 2. Wide angle XRD patterns of (a) MOMR-100, (b) MOMR, (c) MOMR-SO_3H, and (d) MOMC-SO_3H.

2. Experimental

2.1. Chemicals and preparation

All reagents were analytical grade. Phenol, formaldehyde solution (38 wt.%), NaOH, ethanol, ferric chloride, ferrous sulfate, sulfuric acid fuming, acetic acid, butanol, cyclohexanol, benzaldehyde, ethylene glycol and dodecane were obtained from Tianjin Guangfu Chemical Company. P123 and Amberlyst 15 were purchased from Sigma-Aldrich Company.

Magentically active ordered mesoporous resin (MOMR) was prepared from hydrothermal synthesis under basic conditions. As a typical run, 0.2 g of NaOH was dissolved in 10 mL of H_2O, followed by addition of 2.0 g phenol and 7 mL formaldehyde solution (38 wt.%). After heating at 70–80 °C for 30–40 min, 20 mL of P123 (containing 1.75 g of P123) solution was added. After heating at 80 °C for 2 h, the mixture was cooled down to room temperature. Then, the mixture was added dropwise into 20 mL of aqueous solution containing ferric chloride ($FeCl_3\cdot6H_2O$, 0.44 mmol) and ferrous sulfate ($FeSO_4\cdot7H_2O$, 0.88 mmol) under vigorous stirring. After further stirring for 30 min, the mixture was transferred to an autoclave. When the autoclave was treated at 180 °C for 24 h, a black precipitate of MOMR was obtained. When heating at 600 °C for 2 h in flowing N_2 for carbonization, magnetically active ordered mesoporous carbon (MOMC) was obtained. Sulfonation of the samples was carried out in a Teflon-lined autoclave according to the literature [23]. The SO_3H-functionalized MOMR and MOMC

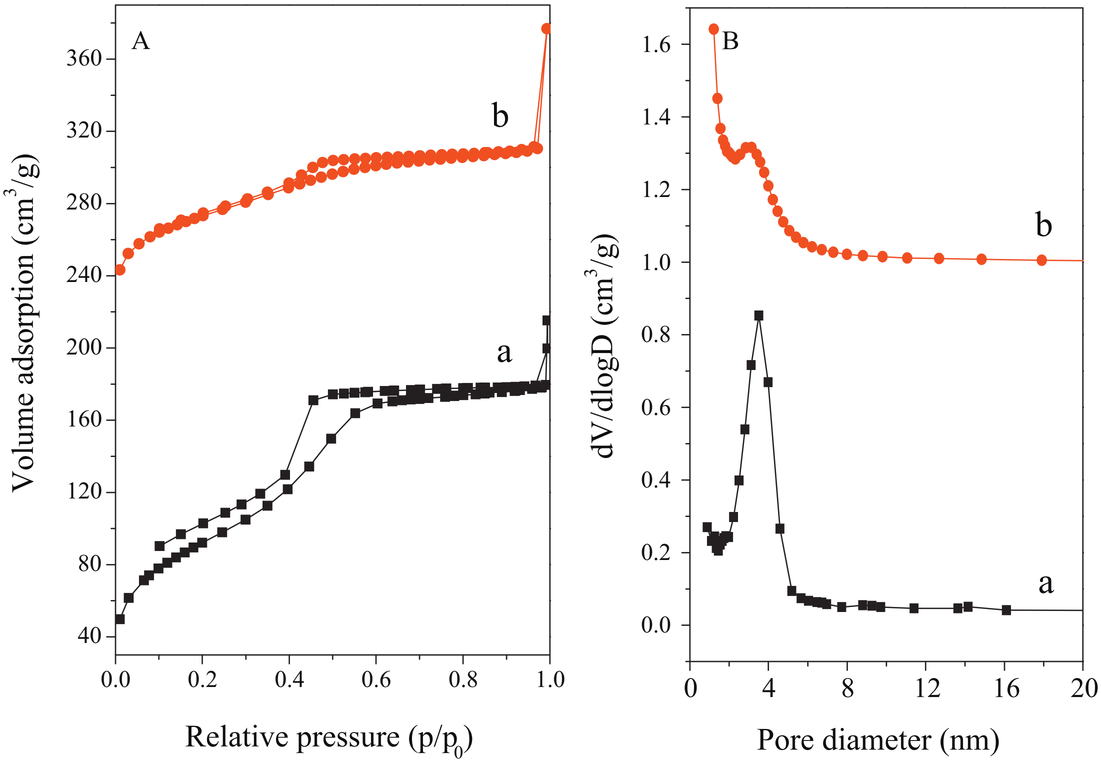

Fig. 3. (A) N_2 isotherms and (B) pore size distributions of (a) MOMR-SO_3H and (b) MOMC-SO_3H. The isotherm for (b) was offset by 100 m^2/g along the vertical axis for clarity, and the pore size distribution for (b) was offset by 1.0 cm^3/g along the vertical axis for clarity.

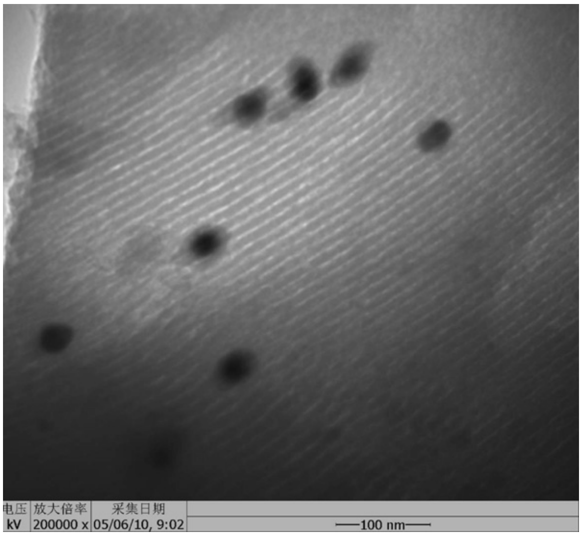

Fig. 4. TEM image of MOMC-SO_3H viewed from (1 1 0) direction.

samples were designated as MOMC-SO_3H and MOMR-SO_3H, respectively.

2.2. Characterization

X-ray diffraction (XRD) patterns were recorded on Rigaku D/Max-2550 (wide-angle XRD) and Siemens D5005 diffractometer (small-angle XRD) using nickel-filtered Cu Kα radiation. N_2 isotherms were measured using a Micromeritics ASAP Tristar system at the liquid nitrogen temperature. The samples were outgassed for 10 h at 150 °C before the measurements. The pore-size distribution for mesopores was calculated using the Barrett–Joyner–Halenda (BJH) model. The magnetization curves were measured at 25 °C under a varying magnetic field with a Quantum Design MPMS-7 SQUID magnetometer. CHNS elemental analysis was performed on a PerkinElmer series II CHNS analyzer 2400. XPS spectra were performed on a Thermo ESCALAB 250 with Al Kα radiation, and binding energies were calibrated using the C1s peak at 284.9 eV. Transmission electron microscopy (TEM) experiments were performed on a JEM-3010 electron microscope (JEOL, Japan) with an acceleration voltage of 300 kV.

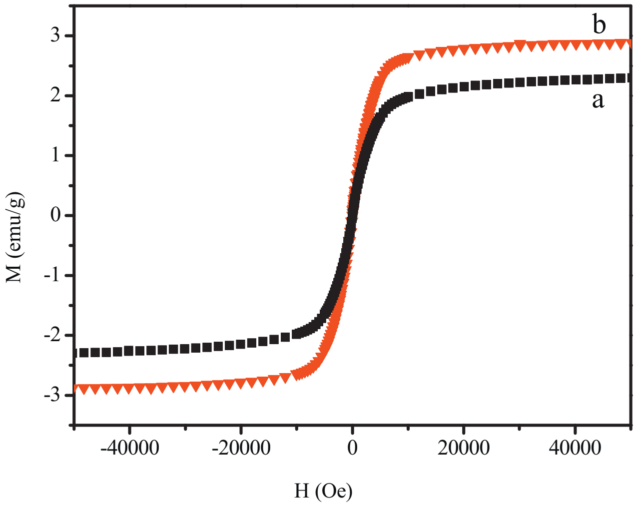

Fig. 5. Magnetization curves of (a) MOMR-SO_3H and (b) MOMC-SO_3H.

2.3. Catalytic reactions

Before catalytic reactions, all catalysts were activated by 0.1 M H_2SO_4 for 4 h at room temperature. Esterification of acetic acid with butanol (EAB) and esterification of acetic acid with cyclohexanol (EAC) as well as condensation of benzaldehyde with ethylene glycol (CBE) were chosen as model reactions. EAB was carried out in a glass flask under vigorous stirring at 90 °C for 4 h with 0.01 g of catalyst, 75 mmol of acetic acid, and 50 mmol of butanol. EAC was carried out in a glass flask under vigorous stirring at 100 °C for 5 h with 0.2 g of catalyst, 305 mmol of acetic acid, and 110 mmol of cyclohexanol. CBE was carried out in a glass flask under vigorous stirring at 90 °C for 1 h with 0.01 g of catalyst, 15 mmol of benzaldehyde, and 15 mmol of ethylene glycol. The products in catalytic reactions were analyzed by gas chromatography (Shimazu 14C) with a

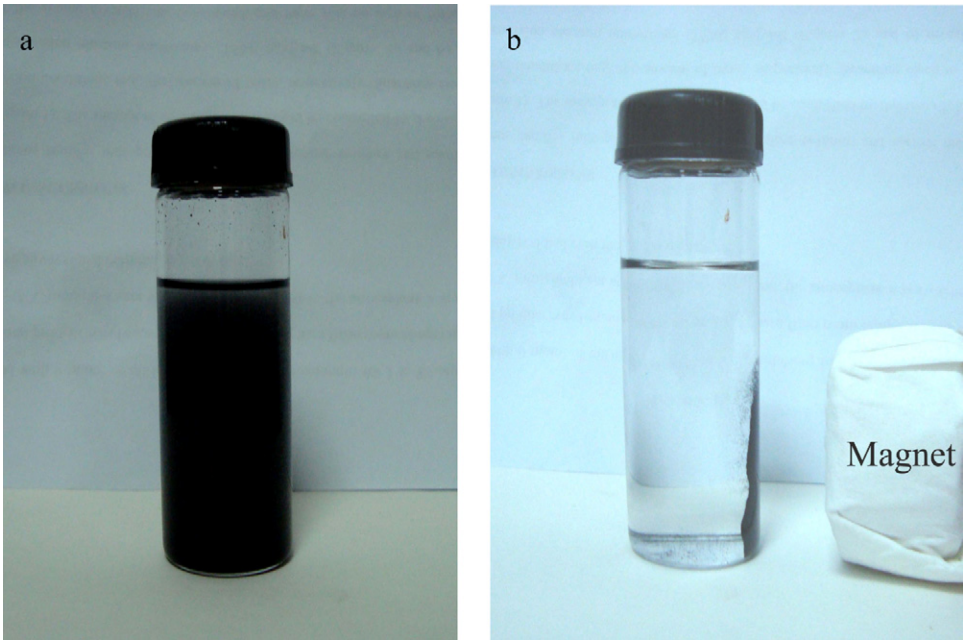

Fig. 6. Photographs of MOMC-SO_3H in ethanol without (a) and with (b) magnetic field.

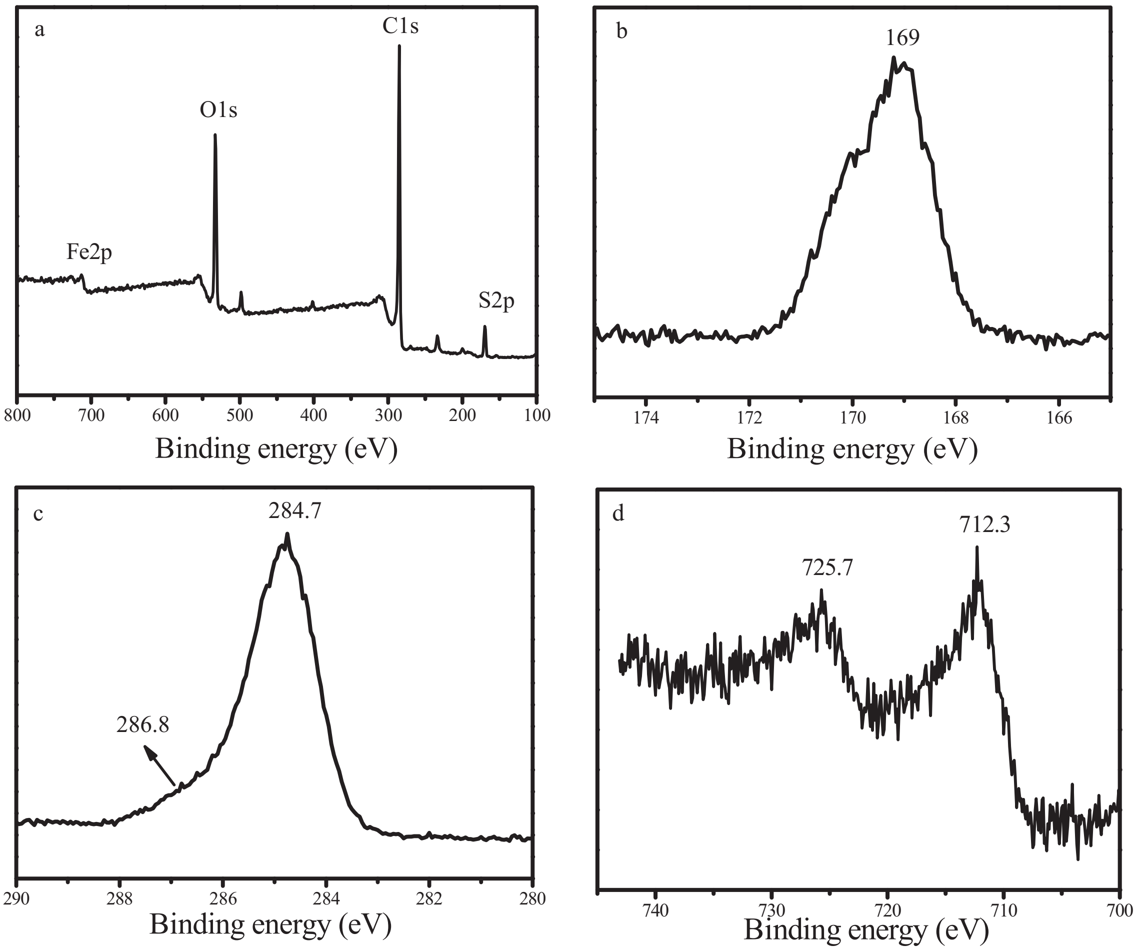

Fig. 7. XPS measurements of (a) survey, (b) S2p, (c) C1s, (d) Fe2p spectra over MOMC-SO_3H.

flame ionization detector (FID), and dodecane was used as an internal standard. The column was OV-1 (30 m), the initial temperature was 100 °C, temperature rate was 20 °C/min, final temperature was 220 °C, and the temperature of FID detector was 280 °C.

3. Results and discussion

3.1. Preparation and characterization

Fig. 1 shows small-angle XRD patterns of MOMR-SO_3H and MOMC-SO_3H samples. Both exhibit two well-resolved peaks indexed as (1 0 0) and (1 1 0) reflections associated with 2-D hexagonal symmetry (*P*6*mm*), indicating their good ordering of mesostructure. Fig. 2 shows wide-angle XRD patterns of mesoporous resin synthesized at 100 °C (MOMR-100), MOMR, MOMR-SO_3H, and MOMC-SO_3H samples. Notably, there is no peak in MOMR-100 sample (Fig. 2a), suggesting the absence of nanocrystals of iron oxides. In contrast, the MOMR and MOMC-SO_3H samples synthesized at 180 °C (Fig. 2b and c) show obvious peaks associated with crystalline γ-Fe_2O_3 [34,36]. After carbonization, the MOMC-SO_3H (Fig. 2d) shows additional peaks associated with α-Fe [33]. The presence of both crystalline γ-Fe_2O_3 and α-Fe is very helpful for preparation of magnetically active composites.

Fig. 3 shows N_2 isotherms and pore size distributions of MOMR-SO_3H and MOMC-SO_3H samples. They show a type-IV isotherm, giving a sharp capillary condensation step at P/P_0 of 0.4–0.6, which is due to the presence of mesoporosity [13–15]. Correspondingly, their pore sizes are distributed at 3.6 and 3.1 nm, respectively. The

Table 1
Textural parameters, sulfur content, and acidic concentration of various solid acid catalysts.

Run	Samples	S_{BET} (m^2/g)	D_p[a] (nm)	V_p (cm^3/g)	S content[b] (mmol/g)	Acid concentration[c] (mmol/g)
1	MOMR-SO_3H	335	3.6	0.35	1.42	1.56
2	MOMC-SO_3H	591	3.1	0.34	0.85	0.91
3	Amberlyst 15	45	40.0	0.31	4.30	4.70
4	SBA-15-SO_3H	820	7.3	1.40	1.26	1.36
5	ZSM-5[d]	364	0.55	0.16	–	–
6	USY[e]	623	14.7	0.26	–	–

[a] Pore size distribution estimated from BJH model.
[b] Measured by elemental analysis.
[c] Measured by acid-base titration.
[d] Si/Al ratio at 40.
[e] Si/Al ratio at 7.5.

pore volumes and BET surface areas of MOMR-SO_3H and MOMC-SO_3H are 0.35 and 0.34 cm^3/g and 335 and 591 m^2/g, as summarized in Table 1. In addition, their sulfur content and acidic concentration were also measured. MOMR-SO_3H and MOMC-SO_3H show the acidic concentration at 1.56 and 0.91 mmol/g, respectively.

Fig. 4 shows a typical TEM image of MOMC-SO_3H viewed from (1 1 0) direction. This image clearly shows not only a good mesostructured ordering but also uniform nanoparticles of iron species including γ-Fe_2O_3 and α-Fe in the carbon network. The particle sizes of iron nanoparticles are mainly ranged at 20–40 nm.

Fig. 5 shows room-temperature magnetization curves of MOMR-SO_3H and MOMC-SO_3H, giving the saturation value at 2.28 and 2.88 emu/g. These results suggest that both samples are magnetically active. Notably, MOMR-SO_3H has the lower value than MOMC-SO_3H, which is related to the formation of α-Fe during carbonization of MOMR (Fig. 2). Furthermore, it is found that both samples have not hysteresis loop, suggesting their superparamagnetic property [36]. Fig. 6 shows photographs of MOMR-SO_3H in ethanol with or without magnetic field. When the magnetic field is absent, the powders of MOMC-SO_3H are highly dispersed in the solution. After introduction of a magnetic filed, the sample powders are easily manipulated by a magnet.

Fig. 7 shows XPS measurement of MOMC-SO_3H, exhibiting the signals of S, C, O, and Fe. The S2p peak at 169.1 eV is assigned to S–O bond, C1s peaks at 284.7 and 286.8 eV are associated with C–C and C–S bonds, and $Fe2p_{3/2}$ and $Fe2p_{1/2}$ peaks at 725.7 and 712.3 eV are mainly attributed to Fe^{3+} species. Fig. 8 shows IR spectra of MOMC and MOMC-SO_3H samples. Interestingly, after sulfonation, MOMC-SO_3H shows additional band at 1032 cm^{-1}, which is characteristic of sulfonic groups in the sample [22]. Both XPS and IR results confirm that sulfonic groups have been successfully functionalized on the surface of ordered mesoporous walls of MOMC-SO_3H.

3.2. Catalytic results

Table 2 presents catalytic data in esterification of acetic acid with butanol (EAB), esterification of acetric acid with cyclohexanol (EAC), and condensation of benzaldehyde with ethylene glycol (CBE). In these reactions, MOMC-SO_3H exhibits much higher activities than zeolites (ZSM-5 and USY) and SO_3H-functionalized on mesoporous silica (SBA-15-SO_3H). Particularly, its activity is even comparable that of Amberlyst 15, one of conventional acidic resins with superior activities. For example, MOMC-SO_3H gives butanol conversion at 96.8% in the EAC (Run 2), which is obviously higher than SBA-15-SO_3H (90.2%, Run 6), ZSM-5 (68.4%, Run 7), and USY (45.8%, Run 8). Because the quite distinguishable acidic sites over various catalysts (Table 1), the turnover numbers of these catalysts are calculated (Table 2). The results show that MOMC-SO_3H (TON of 5318, Run 2) is more active than SBA-15-SO_3H (TON of 3316, Run 6) and Amberlyst 15 (TON of 959, Run 4). The higher activity over MOMC-SO_3H than over SBA-15-SO_3H could be related to the difference in the mesoporous walls that the carbon is more hydrophobic than silica [24], and the higher activity over MOMC-SO_3H than over Amberlyst 15 is reasonably assigned to larger surface area of MOMC-SO_3H than of Amberlyst 15 (Table 1).

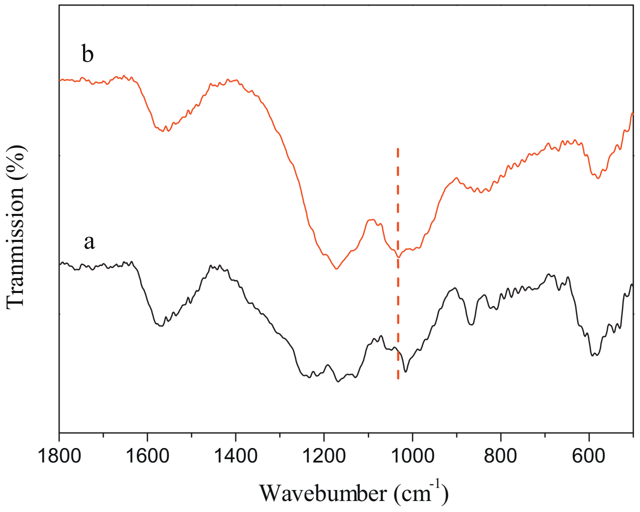

Fig. 8. IR spectra of (a) MOMC-180 and (b) MOMC-SO_3H.

It is worth noting that MOMC-SO_3H shows excellent recyclability (Table 2, Run 3), compared with Amberlyst 15 (Run 5). For example, in the EAB, after recycles for four times, the activity over MOMC-SO_3H is reduced from 96.8% to 92.4%, while the activity over Amberlyst 15 is changed from 99.1% to 90.1% by the same recycling; in the EAC, after recycles for four times, the activity over MOMC-SO_3H is reduced from 60.1% to 54.7%, while the activity over Amberlyst 15 is changed from 59.7% to 35.2% by the same recycling. These results suggest that the sulfonic groups of MOMC-SO_3H are more stable than those of Amberlyst 15 under the same reaction conditions. The analysis of the sample acidic concentration shows MOMC-SO_3H shows that the S element are basically stable after recycles for 4 times (the S content at 0.85 and 0.80 mmol/g for the fresh and recycled sample), in good agreement with those of catalytic results in Table 2.

It is particularly emphasized that MOMC-SO_3H is magnetically active. The combination of high activity, good recyclability, and magnetic movement together would be potentially important for preparing efficient solid acid catalysts for industrial applications.

Table 2
Catalytic data in esterification of acetic acid with butanol (EAB), esterification of acetic acid with cyclohexanol (EAC), and condensation of benzaldehyde with ethylene glycol (CBE) over various solid acid catalysts.

Run	Catalysts	EAB[a]		EAC[b]		CBE[c]	
		Conv. (%)	TON[d]	Conv. (%)	TON[d]	Conv. (%)	TON[d]
1	MOMR-SO_3H	97.6	3128	61.7	218	67.8	807
2	MOMC-SO_3H	96.8	5319	60.1	363	65.9	1086
3	MOMC-SO_3H[e]	92.4	5077	54.7	331		
4	Amberlyst 15	99.1	1054	59.7	70	64.2	207
5	Amberlyst 15[e]	90.1	959	35.2	41		
6	SBA-15-SO_3H	90.2	3316	45.7	185	46.7	515
7	ZSM-5	68.4	8340	19.5	255	43.9	1568
8	USY	45.8	996	39.8	95	39.1	255

[a] The activities in EAB were evaluated by butanol conversion, and the product was butyl acetate with the selectivity higher than 99.9%.
[b] The activities in EAC were evaluated by cyclohexanol conversion, and the product was cyclohexyl acetate with the selectivity higher than 99.9%.
[c] The activities in CBE were evaluated by benzaldehyde conversion, and the product was 2-phenyl-1,3-dioxolane with the selectivity higher than 99.9%.
[d] Number of converted reactant per acidic site in the catalysis.
[e] Recycles for four times.

4. Conclusions

Magnetically active and SO_3H-functionalized ordered mesoporous carbon (MOMC-SO_3H) has been hydrothermally synthesized by self-assembly of resol with triblock polymer (P123) in the presence of iron species at 180 °C, followed by calcination in flowing nitrogen at 600 °C and sulfonation by fuming sulfuric acid. Catalytic tests in esterification and condensation show that MOMC-SO_3H is highly active and excellently recyclable. Particularly, the combination of superior catalytic performance with magnetic activity over MOMC-SO_3H might open an alternative route for designing novel solid acid catalysts for production of fine chemicals by green or sustainable routes.

Acknowledgements

This work is supported by the State Basic Research Project of China (2009CB623507) and National Natural Science Foundation of China (20973079).

References

[1] A. Corma, Chem. Rev. 97 (1997) 2373–2420.
[2] M.E. Davis, Nature 417 (2002) 813–821.
[3] J.H. Clark, D.J. Macquarrie, Chem. Soc. Rev. 25 (1996) 303–310.
[4] A. Corma, Chem. Rev. 95 (1995) 559.
[5] T. Okuhara, Chem. Rev. 102 (2002) 3641–3666.
[6] J.A. Melero, G.D. Stucky, R.V. Griekena, G. Morales, J. Mater. Chem. 12 (2002) 1664–1670.
[7] M.A. Harmer, Q. Sun, Catal. Appl. A 275 (2004) 247–255.
[8] J.A. Dias, J.P. Osegovic, R.S. Drago, J. Catal. 183 (1999) 83–90.
[9] G. Busca, Chem. Rev. 107 (2007) 5366–5410.
[10] T. Welton, Chem. Rev. 99 (1999) 2071–2083.
[11] A. Corma, H. Garcia, Chem. Rev. 103 (2003) 4307–4365.
[12] Y.X. Wei, Y.L. He, D.Z. Zhang, L. Xu, S.H. Meng, Z.M. Liu, B.L. Su, Microporous Mesoporous Mater. 90 (2006) 188–197.
[13] C.T. Kresge, M.E. Leonowicz, W.J. Roth, J.C. Vartuli, J.S. Beck, Nature 359 (1992) 710–712.
[14] D.Y. Zhao, J.L. Feng, Q.S. Huo, N. Melosh, G.H. Fredrickson, B.F. Chmelka, G.D. Stucky, Science 279 (1998) 548–552.
[15] D.Y. Zhao, Q.S. Huo, J.L. Feng, B.F. Chmelka, G.D. Stucky, J. Am. Chem. Soc. 120 (1998) 6024–6036.
[16] V. Dufaud, M. Davis, J. Am. Chem. Soc. 125 (2003) 9403–9413.
[17] D. Margolese, J.A. Melero, S.C. Christiansen, B.F. Chmelka, G.D. Stucky, Chem. Mater. 12 (2000) 2448–2459.
[18] I. Díaz, C. Márquez-Alvarez, F. Mohino, J. Pérez-Pariente, E. Sastre, J. Catal. 193 (2000) 283–294.
[19] I. Díaz, C. Márquez-Alvarez, F. Mohino, J. Pérez-Pariente, E. Sastre, J. Catal. 193 (2000) 295–302.
[20] Q.H. Yang, J. Liu, J. Yang, M.P. Kapoor, S. Inagaki, C. Li, J. Catal. 228 (2004) 265–272.
[21] Z.T. Zhang, Y. Han, L. Zhu, R.W. Wang, Y. Yu, S.L. Qiu, D.Y. Zhao, F.-S. Xiao, Angew. Chem. Int. Ed. 40 (2001) 1258–1262.
[22] R. Xing, N. Liu, Y.M. Liu, H.H. Wu, Y.W. Jiang, L. Chen, M.Y. He, P. Wu, Adv. Funct. Mater. 17 (2007) 2455–2461.
[23] F.-J. Liu, X.-J. Meng, Y.L. Zhang, L.M. Ren, F. Nawaz, F.-S. Xiao, J. Catal. 271 (2010) 52–58.
[24] M. Hara, T. Yoshida, A. Takagaki, T. Takata, J.N. Kondo, S. Hayashi, K. Domen, Angew. Chem. Int. Ed. 43 (2004) 2955–2958.
[25] X.Q. Wang, R. Liu, M.M. Waje, Z.W. Chen, Y.S. Yan, K.N. Bozhilov, P.Y. Feng, Chem. Mater. 19 (2007) 2395–2397.
[26] R. Xing, Y.M. Liu, Y. Wang, L. Chen, H.H. Wu, Y.W. Jiang, M.Y. He, P. Wu, Microporous Mesoporous Mater. 105 (2007) 41–48.
[27] Y.J. Xu, W.Q. Gu, D.L. Gin, J. Am. Chem. Soc. 126 (2004) 1616–1617.
[28] J. Janaun, N. Ellis, Appl. Catal. A 394 (2011) 25–31.
[29] C.D. Liang, Z.J. Li, S. Dai, Angew. Chem. Int. Ed. 47 (2008) 3696–3717.
[30] C. Liang, S. Dai, J. Am. Chem. Soc. 128 (2006) 5316–5317.
[31] Y. Meng, D. Gu, F.Q. Zhang, Y.F. Shi, H.F. Yang, Z. Li, C.Z. Yu, B. Tu, D.Y. Zhao, Angew. Chem. Int. Ed. 44 (2005) 7053–7059.
[32] F.Q. Zhang, Y. Meng, D. Gu, Y. Yan, C.Z. Yu, B. Tu, D.Y. Zhao, J. Am. Chem. Soc. 127 (2005) 13508–13509.
[33] Z.H. Sun, L.F. Wang, P.P. Liu, S.C. Wang, B. Sun, D.Z. Jiang, F.-S. Xiao, Adv. Mater. 18 (2006) 1968–1971.
[34] Y.P. Zhai, Y.Q. Dou, X.X. Liu, B. Tu, D.Y. Zhao, J. Mater. Chem. 19 (2009) 3000–3292.
[35] A.H. Lu, W. Schmidt, N. Matoussevitch, H. Bŏnnemann, B. Spliethoff, B. Tesche, E. Bill, W. Kiefer, F. Schüth, Angew. Chem. Int. Ed. 43 (2004) 4303–4306.
[36] W. Zhao, J. Gu, L. Zhang, H. Chen, J. Shi, J. Am. Chem. Soc. 127 (2005) 8916–8917.
[37] Y. Li, H.Y. Tan, X.Y. Yang, B. Goris, J. Verbeeck, S. Bals, P. Colson, R. Cloots, G. Tendeloo, B.L. Su, Small 7 (2011) 475–483.
[38] R. Xiang, G.H. Luo, W.Z. Qian, Q. Zhang, Y. Wang, F. Wei, Q. Li, A.Y. Cao, Adv. Mater. 19 (2007) 2360–2363.
[39] W. Chen, X.L. Pan, M.G. Willinger, D.S. Su, X.H. Bao, J. Am. Chem. Soc. 128 (2006) 3136–3137.
[40] M.H. Cao, T.F. Liu, S. Gao, G.B. Sun, X.L. Wu, C.W. Hu, Z.L. Wang, Angew. Chem. Int. Ed. 44 (2005) 4197–4201.
[41] F.J. Liu, C.J. Li, L.M. Ren, X.J. Meng, H. Zhang, F.-S. Xiao, J. Mater. Chem. 19 (2009) 7921–7928.